Optics Communications 467 (2020) 125712

Contents lists available at ScienceDirect

Optics Communications

journal homepage: www.elsevier.com/locate/optcom

Adaptive least squares channel estimation for visible light communications based on tap detection

Xiaolin Shi [a,*], Shu-Hung Leung [b], Jie Min [a]

[a] School of Electronic Engineering, Xi'an University of Posts and Telecommunications, Xi'an, China
[b] Department of Electrical Engineering, City University of Hong Kong, Hong Kong, China

ARTICLE INFO

Keywords:
Adaptive channel estimation
Least squares (LS)
Direct current biased optical OFDM (DCO-OFDM)
Visible light communication (VLC)
Tap detection

ABSTRACT

Visible light communication (VLC) is one of the promising technologies for future wireless communications and has attracted increasing research interest in recent years. In this paper, we propose an adaptive least squares (LS) channel estimation algorithm for VLC systems using the direct current biased optical orthogonal frequency division multiplexing (DCO-OFDM) scheme. The proposed algorithm is obtained by employing the tap detection that provides the maximum probability of correctly separating non-zero and zero-value channel taps, yielding significantly improved estimation performance. We prove that the Cramér–Rao lower bound of the proposed algorithm is lower than that of the conventional LS algorithm. Finally, numerical results demonstrate that the proposed algorithm achieves better performance in terms of the received constellation, mean squared error (MSE) and bit error rate (BER).

1. Introduction

The unprecedented increase in various wireless devices and services has led to the congestion of radio frequency (RF) spectrum and an exponentially growing demand for bandwidth and high data rates. To address these issues, visual light communication (VLC) has been developed as a promising alternative technology to RF technologies due to its broad bandwidth and potential in providing very high data rate transmission through the use of solid-state lighting devices [1].

In view of its successful applications in RF communications, orthogonal frequency division multiplexing (OFDM) has been used for mitigating inter-symbol interference (ISI) affected by dispersive channels in optical communications [2]. Unlike the bipolar nature of OFDM signals in RF systems, the adoption of intensity modulation and direct detection (IM/DD) in optical OFDM systems requires the transmitted signals to be real and non-negative [3]. Several multicarrier modulation techniques have been developed for generating real-value unipolar signals over optical channels. The most common approaches include direct current biased optical OFDM (DCO-OFDM) [4–7], asymmetrically clipped optical OFDM (ACO-OFDM) [8,9] and unipolar OFDM (U-OFDM) [10,11]. Due to its spectral efficiency and flexibility, DCO-OFDM has become one of the most commonly used schemes in VLC systems [7].

Channel state information (CSI) must be estimated in order to ensure stable and efficient data transmission in OFDM-based VLC systems. In comparison with RF scenarios, there has been limited considerations on channel estimation for VLC systems. The principles of conventional channel estimation algorithms, for example pilot-aided channel estimation algorithms, are applicable to VLC scenarios [12,13]. Some estimation algorithms for optical channels [14–16] have been developed, where maximum likelihood sequence detection (MLSD) [17] was adopted for mitigating inter-symbol interference (ISI). In [18], the equalization based on linear decision feedback and artificial neural network (ANN) was proposed for VLC, where equalizers were performed in real-time, though at the cost of increased complexity. A discrete Fourier transform (DFT) based channel estimation algorithm for a coherent OFDM transmission system was proposed in [19]. The linear minimum mean squared error (LMMSE) algorithm, a modified algorithm of minimum mean squared error (MMSE), was proven to provide better performance than the LS algorithm in [20]. However, it has extremely large computational complexity and needs to know prior channel statistical information. Since the computational complexities of these algorithms are so large, they are not suitable for practical implementation. Therefore, the least squares (LS) algorithm [7,20] is often applied to obtain the channel impulse response (CIR) in OFDM-based VLC systems due to ease of implementation.

The sparse signal reconstruction algorithm based on compressed sensing (CS) theory, such as orthogonal matching pursuit (OMP), has been applied to solve the channel estimation problem in OFDM-based VLC systems [21]. In [22], a hybrid algorithm based on the least squares discrete Fourier transform (LS-DFT) algorithm and the OMP algorithm (LS-DFT-OMP) was employed to improve the performance of OFDM-based VLC systems, which was on the assumption that the

* Corresponding author.
E-mail address: linda20016@163.com (X. Shi).

https://doi.org/10.1016/j.optcom.2020.125712
Received 30 January 2020; Received in revised form 8 March 2020; Accepted 9 March 2020
Available online 13 March 2020
0030-4018/

communication channel was sparse in discrete time domain. However, the selection on the channel threshold and signal-to-noise ratio (SNR) threshold of the LS-DFT-OMP algorithm comes from experiments and lacks theoretical analysis.

In view of the previous works above, in this paper we propose a new LS channel estimation for DCO-OFDM systems, which is capable of achieving a superior performance in terms of the received constellation, mean square error (MSE) and bit error rate (BER). The main contributions of the paper are summarized as:

(1) An adaptive channel estimation algorithm based on the sparse LS channel estimation and the tap detection is developed, which theoretically maximizes the probability for detecting non-zero and zero-value channel taps. It is shown that the proposed algorithm can achieve better performance than the LS-DFT-OMP algorithm [22].

(2) The Cramér–Rao lower bound (CRLB) of the proposed algorithm is analyzed. The theoretical results show that the proposed algorithm has lower CRLB than that of the conventional LS algorithm [7,20]. Thus, the new algorithm can approach lower MSE.

In this paper, bold variables denote matrices or vectors. $(\cdot)^*$ is the conjugation operation; $[\cdot]_i$ and $[\cdot]_{i,j}$ denote the ith element of a vector and the (i,j)th element of a matrix, respectively; $(\cdot)^T$ and $(\cdot)^H$ represent the transpose and Hermitian transpose operations, respectively; $\mathbf{I}_n(\cdot)$ denotes an n× n identity matrix; diag$\{\cdot\}$ represents a diagonal matrix; $\|\cdot\|_0$ and $\|\cdot\|_2$ represents the ℓ_0- and ℓ_2-norm operations, respectively; The symbol "∼" means "distributed as"; $E\{\cdot\}$ represents the expectation operation; Re$\{z\}$ is the real part of complex number z; and $(\hat{x})$ denotes the estimate of variable x.

2. VLC system model

A general DCO-OFDM system with N_s subcarriers for parallel transmission is considered in Fig. 1. In the system, the bit stream of input data is mapped to constellation points of an M-ary modulation scheme, namely, multilevel phase shift keying (M-PSK), multilevel pulse amplitude modulation (M-PAM), or multilevel quadrature amplitude modulation (M-QAM). The transmitted signal in frequency domain, represented by the $N_s \times 1$ vector $\mathbf{X}$, is composed of N_d data and N_p pilot symbols, where $N_s = N_d + N_p$. Since IM/DD signals have real and non-negative values, the elements $\{X[k]\}$ of $\mathbf{X}$ are constrained to be Hermitian symmetric as [3,6]

$$X[k] = X^*\left[N_s - k\right], \quad 0 \le k \le N_s/2, \tag{1}$$

where $X[0] = X^*\left[N_s/2\right] = 0$. After the inverse fast Fourier transform (IFFT) operation and the addition of the cyclic prefix (CP), the resultant transmitted signal is converted to its optical version and then transmitted through the optical channel.

At the receiver, after the removal of the CP and the fast Fourier transform (FFT) operation, the received signal at the kth subcarrier is given by

$$y[k] = R_{pd} H[k] X[k] + N[k], \quad k = 0, \ldots, (N_s - 1), \tag{2}$$

where R_{pd} is the photodetector (PD) responsivity in Ampere/Watt (A/W), $H[k]$ and $X[k]$ are the VLC channel gain and the transmitted symbol at the kth subcarrier, respectively, $N[k]$ is an additive white Gaussian noise (AWGN) representing the shot and thermal noise suffered by the VLC system [23]. The noise samples $\{N[k]\} \sim CN(0, \sigma_n^2)$ are independent identically distributed Gaussian random variables. Therefore, the received signal in vector form can be expressed as

$$\boldsymbol{y} = R_{pd} \mathrm{diag}\{\mathbf{X}\}\mathbf{H} + \mathbf{N} = R_{pd}\mathrm{diag}\{\mathbf{X}\}\mathbf{F}\mathbf{h} + \mathbf{N}, \tag{3}$$

where $\boldsymbol{y}$ and $\mathbf{N}$ are $N_s \times 1$ vectors composed of the received symbols and the AWGN, respectively, diag$\{\mathbf{X}\}$ is an $N_s \times N_s$ diagonal matrix whose diagonal is the transmitted signal $\mathbf{X}$, $\mathbf{H} = \mathbf{F}\mathbf{h}$ is the channel vector in frequency domain, $\mathbf{F}$ is the $N_s \times L$ DFT matrix whose (n,l)th element is $[\mathbf{F}]_{n,l} = e^{-j\frac{2\pi nl}{N}}$, and $\mathbf{h} = [h(0), h(1), \ldots, h(L-1)]^T$ is the CIR with the maximum tap number L.

Given that the transmitted signal $\mathbf{X}$ is composed of data and pilots, the received pilot signal can be expressed as

$$\boldsymbol{r} = R_{pd} \mathrm{diag}\{\mathbf{P}\}\mathbf{F}_p\mathbf{h} + \mathbf{n}, \tag{4}$$

where $\boldsymbol{r}$ is the $N_p \times 1$ received pilot vector. $\mathbf{n} \sim CN(\mathbf{0}, \sigma_n^2 \mathbf{I}_{N_p})$ is the $N_p \times 1$ noise vector, which is independent of $\mathbf{h}$. diag$\{\mathbf{P}\}$ is the $N_p \times N_p$ diagonal matrix of the pilot signal $\mathbf{P}$, and $\mathbf{F_p}$ is an $N_p \times L$ matrix formed by the N_p rows of the DFT matrix $\mathbf{F}$ in (3) corresponding to the pilots. It is assumed that the channel taps $\{h(i)\}$ are independent zero mean Gaussian random variables with $h(i) \sim N(0, p_i)$, where p_i is the variance of the ith channel tap.

3. Proposed channel estimation

3.1. Sparse LS channel estimation

The channel estimate obtained by the conventional LS algorithm [7,20] is expressed as

$$\hat{\mathbf{h}}_{LS} = \mathrm{Re}\{\underset{\mathbf{h}}{\mathrm{argmin}}\left\|\mathbf{r} - R_{pd}\mathbf{A}\mathbf{h}\right\|_2^2\} = \mathrm{Re}\{\frac{1}{R_{pd}}\left(\mathbf{A}^H\mathbf{A}\right)^{-1}\mathbf{A}^H\mathbf{r}\}, \tag{5}$$

where $\mathbf{A} = \mathrm{diag}\{\mathbf{P}\}\mathbf{F}_p$. However, the estimation performance of the conventional LS algorithm on sparse channels is not that satisfactory because it does not consider the sparse characteristic of optical channels [22]. Thus, a position vector $\mathbf{b}$ is introduced to describe the positions of sparse channel taps, whose elements are given by

$$b_i = \begin{cases} 1, & i \in \mathcal{B} \\ 0, & i \notin \mathcal{B} \end{cases}, \tag{6}$$

where $\mathcal{B} = (i_0, i_1, \ldots, i_{\|\mathbf{h}\|_0 - 1})$ represents the position set with $\|\mathbf{h}\|_0$ non-zero channel taps. For the sparse channel, we have $1 < \|\mathbf{h}\|_0 \ll L$. Then, the received pilot signal in (4) can be rewritten as

$$\mathbf{r} = R_{pd}\mathbf{A}\mathrm{diag}\left\{\hat{\mathbf{b}}\right\}\mathbf{h} + \mathbf{n}. \tag{7}$$

The channel estimate obtained by the sparse LS method can be expressed as [24]

$$\hat{\mathbf{h}}_{SLS} = \mathrm{Re}\{\frac{1}{R_{pd}}\left(\mathbf{S}_A{}^H\mathbf{S}_A\right)^{\dagger}\mathbf{S}_A{}^H\mathbf{r}\}, \tag{8}$$

where $\mathbf{S}_A = \mathbf{A}\mathrm{diag}\left\{\hat{\mathbf{b}}\right\}$, and $(\mathbf{M})^\dagger$ denotes the pseudo-inverse operation of matrix $\mathbf{M}$. Due to the sparse nature of $\hat{\mathbf{b}}$, the matrix $\mathbf{S}_A$ is not full-rank. Therefore, the pseudo-inverse operation is required in (8). Substituting (7) into (8), the sparse channel estimate can be rewritten as

$$\hat{\mathbf{h}}_{SLS} = \mathbf{h} + \mathrm{Re}\{\frac{1}{R_{pd}}\mathbf{S}_A^\dagger\mathbf{n}\} = \mathbf{h} + \mathbf{v}, \tag{9}$$

where $\mathbf{v} = \mathrm{Re}\{\frac{1}{R_{pd}}\mathbf{S}_A^\dagger\mathbf{n}\}$ represents the $L \times 1$ zero mean AWGN vector with the covariance matrix of $\mathbf{v}$ expressed as $E\left[\mathbf{v}\mathbf{v}^H\right] = \sigma_v^2\mathbf{I}_L$, i.e., $\mathbf{v} \sim N(\mathbf{0}, \sigma_v^2\mathbf{I}_L)$. The noise vector $\mathbf{v}$ is independent of $\mathbf{h}$. The ith element of $\hat{\mathbf{h}}_{SLS}$ can be expressed as

$$\hat{h}_{SLS,i} = \begin{cases} h_i + v_i, & i \in \mathcal{B} \\ v_i, & i \notin \mathcal{B} \end{cases}. \tag{10}$$

As clearly expressed in Eqs. (9) and (10), the sparse channel estimate, $\hat{\mathbf{h}}_{SLS}$, is the sum of the actual CIR and the AWGN, where the ith channel tap estimate is either $(h_i + v_i)$ or v_i for $i = 0, 1, \ldots, (L-1)$. Due to the characteristic of the estimate, a channel tap detection scheme needs to be developed for identifying non-zero and zero-value channel taps.

3.2. Tap detection scheme

The detection problem is essentially to choose between the two hypotheses, which are defined as

$$\begin{aligned} H_1 &: \ \hat{h}_{SLS,i} = h_i + v_i \\ H_0 &: \ \hat{h}_{SLS,i} = v_i \end{aligned}. \tag{11}$$

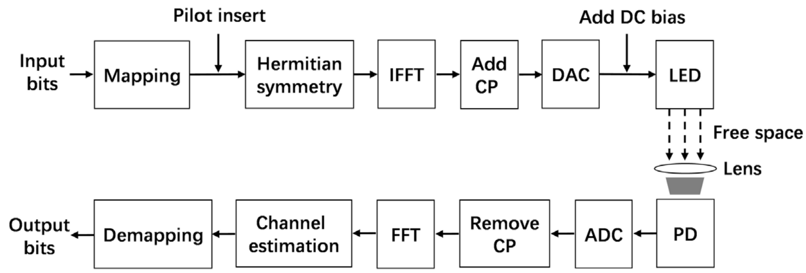

Fig. 1. The schematic diagram of a typical DCO-OFDM system.

Under hypothesis $H_1, \hat{h}_{SLS,i} = h_i + v_i$ is a zero mean Gaussian random variable with variance $\sigma^2_{\hat{h}_{SLS,i}|H_1} = p_i + \sigma_v^2$, since h_i and v_i are independent Gaussian random variables. On the other hand, under hypothesis $H_0, \hat{h}_{SLS,i} = v_i$ is a zero mean Gaussian random variable with variance $\sigma^2_{\hat{h}_{SLS,i}|H_0} = \sigma_v^2$. In the proposed detection scheme, a threshold T is compared with the instantaneous energy of $\hat{h}_{SLS,i}$ in (10). If the instantaneous energy of $\hat{h}_{SLS,i}$ is larger than T, the corresponding channel tap is a non-zero tap, i.e., H_1 is true; otherwise, it is a zero-value tap, i.e. H_0 is true. In other words, the two hypotheses can be rewritten as

$$\begin{aligned} H_1 &: \hat{h}^2_{SLS,i} > T \\ H_0 &: \hat{h}^2_{SLS,i} < T \end{aligned} . \tag{12}$$

The probability density functions of $\hat{h}^2_{SLS,i}$ under the two hypotheses are respectively expressed as

$$f_{\hat{h}^2_{SLS,i}|H_1}(u) = \frac{1}{\sqrt{2\pi u(p_i + \sigma_v^2)}} e^{-\frac{u}{2(p_i+\sigma_v^2)}}, \quad u > 0, \tag{13}$$

$$f_{\hat{h}^2_{SLS,i}|H_0}(u) = \frac{1}{\sqrt{2\pi u \sigma_v^2}} e^{-\frac{u}{2\sigma_v^2}}, \quad u > 0. \tag{14}$$

The objective function for the design of the threshold T_i for the ith channel tap is defined as

$$T_{opt,i} = \underset{T}{\operatorname{argmin}}\{P_{e,i} = \Pr\left(H_0|H_1\right)\Pr\left(H_1\right) + \Pr\left(H_1|H_0\right)\Pr\left(H_0\right)\}, \tag{15}$$

where $\Pr\left(H_1\right)$ and $\Pr\left(H_0\right)$ are the prior probabilities of H_1 and H_0, respectively. $\Pr\left(H_i|H_j\right)$ is the conditional probability of H_i with respect to H_j. $\Pr\left(H_0|H_1\right)$ and $\Pr\left(H_1|H_0\right)$ are respectively expressed as

$$\Pr\left(H_0|H_1\right) = \int_0^T f_{\hat{h}^2_{SLS,i}|H_1}(u)du, \tag{16}$$

$$\Pr\left(H_1|H_0\right) = \int_T^\infty f_{\hat{h}^2_{SLS,i}|H_0}(u)du. \tag{17}$$

Let $P_1 = \Pr\left(H_1\right)$ and $P_0 = \Pr\left(H_0\right)$. The ratio $S = \frac{P_0}{P_1}$ can be viewed as the sparsity of the channel.

The objective is equivalent to minimizing the probability of error in the tap detection.

The optimal $T_{opt,i}$ can be obtained by minimizing $P_{e,i}$ with respect to T. Differentiating $P_{e,i}$ with respect to T and setting the derivative to zero gives

$$T_{opt,i} = \frac{2(p_i + \sigma_v^2)\sigma_v^2}{p_i} \log\left(S\frac{\sqrt{p_i + \sigma_v^2}}{\sigma_v}\right). \tag{18}$$

In Eq. (18), p_i, σ_v^2, and S are usually unknown in practical cases. Therefore, we propose to obtain p_i, $\hat{\sigma}_v^2$, and S from $\hat{\mathbf{h}}_{SLS}$ and $\hat{\mathbf{b}}$ as

$$\hat{\sigma}_v^2 = \frac{1}{(L-D)}[\hat{\mathbf{h}}_{SLS} - \operatorname{diag}(\hat{\mathbf{b}})\hat{\mathbf{h}}_{SLS}]^H[\hat{\mathbf{h}}_{SLS} - \operatorname{diag}(\hat{\mathbf{b}})\hat{\mathbf{h}}_{SLS}], \tag{19}$$

$$p_i = \max\left[\left(\hat{h}_{SLS,i}\right)^2 - \hat{\sigma}_v^2, 0\right], \tag{20}$$

$$S = \frac{L-D}{D}, \tag{21}$$

where $D = \sum_{i=0}^{L-1} \hat{b}_i$, and $\max\left[a_1, a_2\right]$ represents the operation to select the maximum value out of a_1 and a_2.

Similar to the conventional LS algorithm, the proposed adaptive LS algorithm is also able to offer a simple and effective channel estimation for VLC systems. It is worth mentioning that the proposed algorithm just requires the information of the received signal and the knowledge of pilots at the receiver, and the method can be easily extended to other optical OFDM-based systems, such as ACO-OFDM and U-OFDM. The proposed algorithm is summarized in Algorithm 1.

Algorithm 1: Adaptive LS channel estimation based on tap detection

1. **Initialization:**
   Obtain the initial channel estimate $\hat{\mathbf{h}}^{(0)}_{SLS} = \hat{\mathbf{h}}_{LS}$, and set $\hat{\mathbf{b}} = 0$, $l = 0$, $S = 1$.
   Calculate $\hat{\sigma}_v^2$ and p_i by (19) and (20), respectively.
   Compute the optimal threshold $T_{opt,i}$ by (18).
2. **Repeat**
3. Calculate $\hat{\mathbf{h}}^{(l)}_{SLS}$ by (8).
4. Make the hard decision on $\hat{h}^{(l)}_{SLS,i}$ by $T_{opt,i}$ and calculate the tap position by
   $\hat{b}_i = 0.5 \times \left[\operatorname{sign}\left(\left(\hat{h}^{(l)}_{SLS,i}\right)^2 - T_{opt,i}\right) + 1\right]$.
5. Calculate $D = \sum_{i=0}^{L-1} \hat{b}_i$ and the sparsity $S = \frac{L-D}{D}$.
6. Calculate $\hat{\sigma}_v^2$ and p_i by (19) and (20), respectively.
7. Calculate the optimal threshold $T_{opt,i}$ by (18).
8. $l = l + 1$
9. **until** $||\hat{\mathbf{h}}^{(l)}_{SLS} - \hat{\mathbf{h}}^{(l-1)}_{SLS}||_2^2 < \varepsilon$
10. **Return:** $\hat{\mathbf{h}}^{(l)}_{SLS}$

3.3. CRLB analysis

To evaluate the estimation performance of the proposed algorithm, its CRLB, the minimum MSE, is derived and compared with that of the conventional LS algorithm. In the proposed algorithm, non-zero channel taps are more accurately estimated after the exclusion of zero-value channel taps. Therefore, the CRLB of the proposed algorithm, C_{SLE}, can be given by [25]

$$C_{SLE} = \operatorname{CRLB}(\mathbf{h}|\mathcal{B}) = \operatorname{trace}\left[\mathbf{I}^{-1}_{FI}(\mathbf{h}|\mathcal{B})\right], \tag{22}$$

where trace[$\cdot$] represents the trace operation and $\mathbf{I}_{FI}$ represents the Fisher information matrix whose (i,j)th element is expressed as [25]

$$[\mathbf{I}_{FI}(\mathbf{h}|\mathcal{B})]_{i,j} = -E\left[\frac{\partial^2 \log[p(\mathbf{r}|\mathbf{h},\mathcal{B})]}{\partial h_i \partial h_j}\right], \tag{23}$$

where $\log[p(\mathbf{r}|\mathbf{h},\mathcal{B})]$ is the log-likelihood function of the received pilot signal, as given by

$$\log[p(\mathbf{r}|\mathbf{h},\mathcal{B})] = -\frac{N_p}{2}\log(2p\sigma_n^2) - \frac{1}{2\sigma_n^2}\|\mathbf{r} - R_{pd}\mathbf{A}_{\mathcal{B}}\mathbf{h}\|_2^2. \tag{24}$$

Substituting (24) into (23), we obtain

$$\mathbf{I}_{FI}(\mathbf{h}|\mathcal{B}) = R_{pd}^2 \mathbf{A}_{\mathcal{B}}^{\mathrm{H}}\mathbf{A}_{\mathcal{B}}/\sigma_n^2. \tag{25}$$

Assume that the pilots are uniformly distributed in frequency domain, $\mathbf{A}$ satisfies $\mathbf{A}^H\mathbf{A} = N_p\mathbf{I}_L$ and $\operatorname{trace}[(\mathbf{A}^H_{\mathcal{B}}\mathbf{A}_{\mathcal{B}})^{-1}] = \|\mathbf{h}\|_0/N_p$. Therefore,

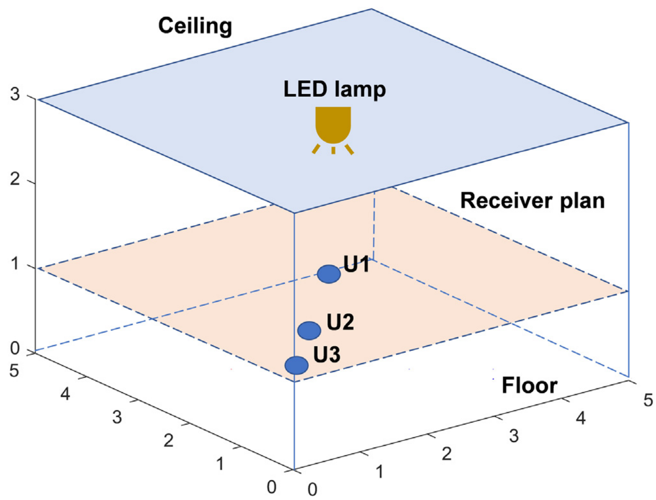

Fig. 2. A typical indoor VLC environment.

the CRLB of the proposed algorithm in (22) can be rewritten as

$$C_{SLE} = \frac{\sigma_n^2}{R_{pd}^2}\text{trace}\left[(\mathbf{A}_B^{\mathrm{H}}\mathbf{A}_B)^{-1}\right] = \frac{\sigma_n^2\|\boldsymbol{h}\|_0}{R_{pd}^2 N_p}. \tag{26}$$

For the sparse channel, $1 \le \|\boldsymbol{h}\|_0 \ll L$. Thus, the range of the CRLB of the proposed algorithm is given by

$$\frac{\sigma_n^2}{R_{pd}^2 N_p} \le C_{SLE} < \frac{\sigma_n^2 L}{R_{pd}^2 N_p}. \tag{27}$$

Similarly, the CRLB of the conventional LS algorithm is given by

$$C_{LE} = \frac{\sigma_n^2}{R_{pd}^2}\text{trace}\left[(\mathbf{A}^H\mathbf{A})^{-1}\right] = \frac{\sigma_n^2 L}{R_{pd}^2 N_p}. \tag{28}$$

It can be observed from (27) and (28) that the CRLB of the proposed algorithm is obviously less than that of the conventional LS algorithm, i.e., $C_{SLE} < C_{LE}$. Furthermore, if all the channel taps have non-zero values, the performance of the proposed algorithm will worsen and is even inferior to the conventional LS algorithm.

4. Results and discussion

In this section, simulation results are provided for demonstrating the effectiveness of the proposed channel estimation algorithm. Let us consider a typical indoor environment shown in Fig. 2, where the room size is $5\times5\times3$ m^3. A lamp of light-emitting diodes (LEDs) is located at the center of the ceiling, which is assumed to have a fixed transmission power and forms a square-shaped coverage area for both illumination and communication services. The user equipment (UE) uses a single PD to receive signals sent from the LED lamp and is placed at a height of 1 m from the ground, which would be the case that a laptop computer uses VLC links for Internet connection. The layout of both the ceiling and the UE plan in the room is shown in Fig. 3, and three different positions of the UE are also marked in the figure as U1, U2 and U3. In the following simulations, parameters are selected as shown in Table 1.

Table 1
Major parameters for experiments.

Parameter	Value	Unit
Room size	$5\times5\times3$	m^3
Reflection coefficient (wall/floor/ceiling)	0.8	–
PD responsivity R_{pd}	0.54	A/W
DC bias	13	dB
Detector area	1	cm^2
Sampling rate	500	MHz
Modulation format	16-QAM	–
Semi-half power angle	60	degree
Field of view at receiver	85	degree
Number of subcarriers	1024	–
Pilot interval in frequency domain	32	–
CP length	64	
Maximum tap delay	30	ns

4.1. CIRs and received constellations

The CIR changes with the variations of the UE position. Fig. 4 represents the continuous CIRs measured at three different UE positions marked in Figs. 2 and 3 as U1, U2 and U3. The estimated CIRs obtained by the proposed algorithm are also plotted in Fig. 4 for $SNR = 20$ dB, where SNR is defined as $10\times\log_{10}\{\mathrm{E}\left[\mathbf{X}^H\mathbf{X}\right]/\sigma_n^2\}$. It can be seen from Fig. 4 that the estimated CIRs closely match with the continuous CIRs.

Fig. 5 shows the received constellations by using different channel estimation algorithms for the VLC system. It is observed that the proposed algorithm has a clearer constellation than the LS-DFT-OMP algorithm. In all the simulation experiments, the channel threshold and the SNR threshold in the LS-DFT-OMP algorithm, as suggested in [22], are set to 0.5 and 15 dB, respectively.

4.2. MSE and BER performances

Figs. 6 and 7 show the MSE and BER performances of the LS-DFT-OMP and proposed algorithms at the position of U2. The MSE is defined as MSE (dB) = $10\times\log_{10}\left(\sum_{n=1}^{N_m}\|\mathbf{h}-\hat{\mathbf{h}}\|^2/N_m\right)$, where N_m, set to 1000 for simulation trials, represents the total number of Monte Carlo iterations. In addition, the CRLBs of both algorithms respectively calculated by Eq. (26) and Eq. (28) are also plotted in Fig. 6 for comparisons. The simulation results show that the proposed algorithm achieves better

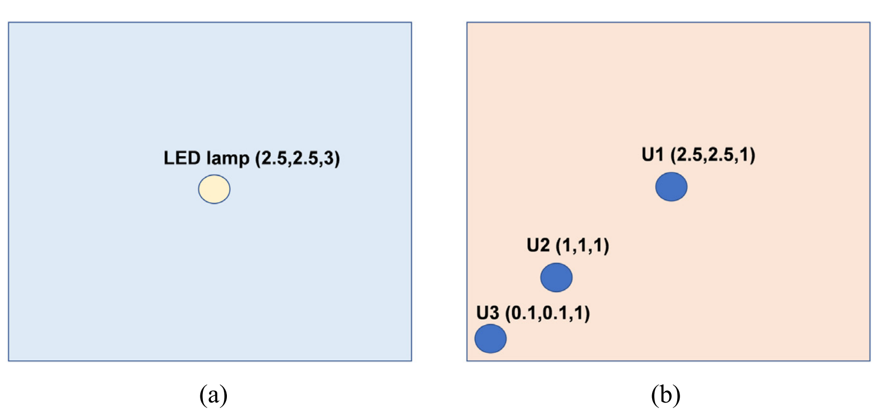

Fig. 3. The layout of ceiling and UE plan: (a) The position of LED lamp (b) three different UE positions.

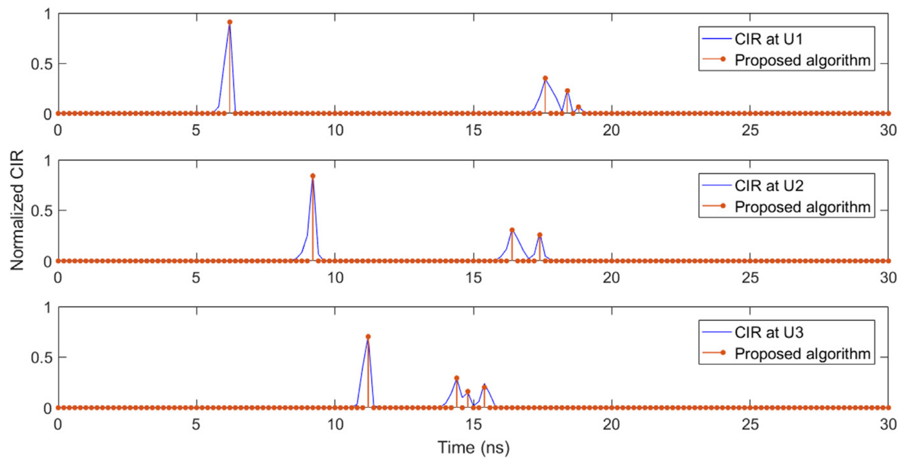

Fig. 4. CIRs for different UE positions.

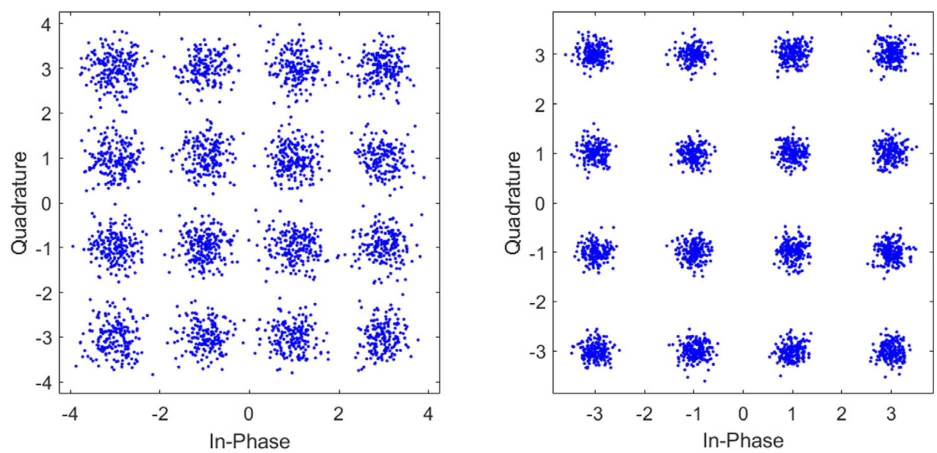

(a) (b)

Fig. 5. The received constellations for SNR=20dB: (a) LS-DFT-OMP (b) Proposed algorithm.

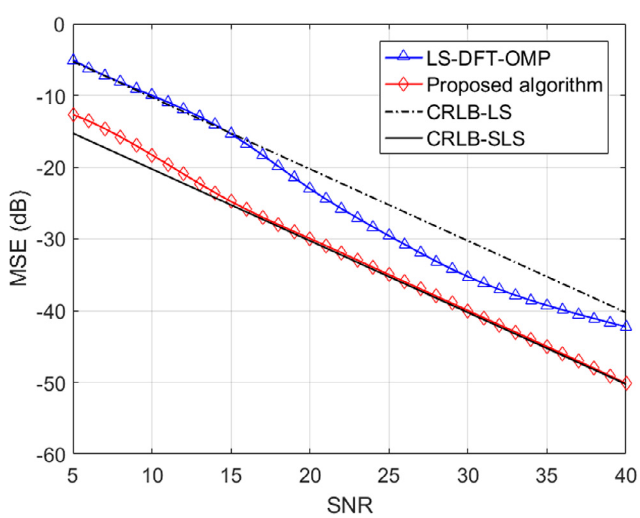

Fig. 6. MSE performances for the position of U2.

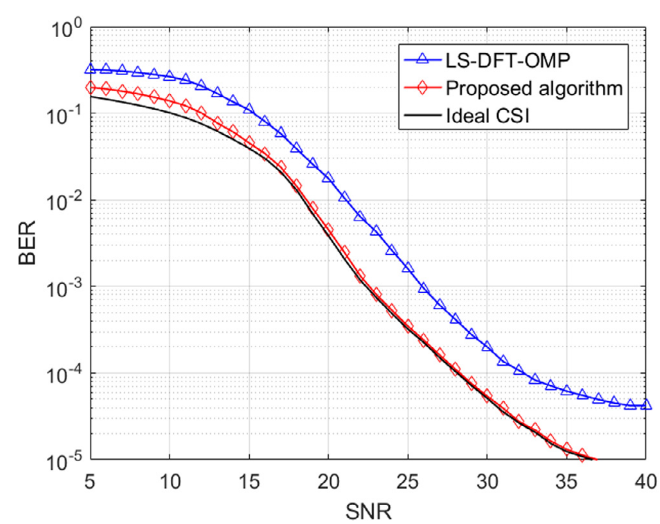

Fig. 7. BER performances for the position of U2.

performance than the LS-DFT-OMP algorithm and gets closer to the ideal performance as SNR increases.

Figs. 8 and 9 show the MSE and BER performances of the LS-DFT-OMP and proposed algorithm versus different UE positions. It can be seen from Figs. 8 and 9 that the proposed algorithm provides the best and stable performances at different UE positions while the LS-DFT-OMP algorithm yields worse and more fluctuant performances. This

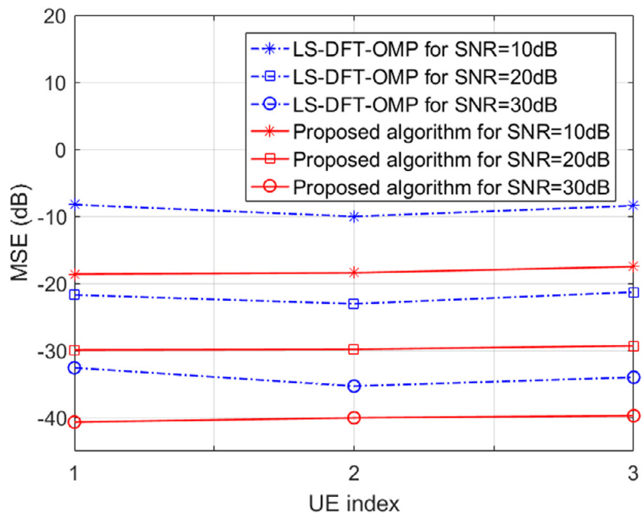

Fig. 8. MSE performances for different UE positions.

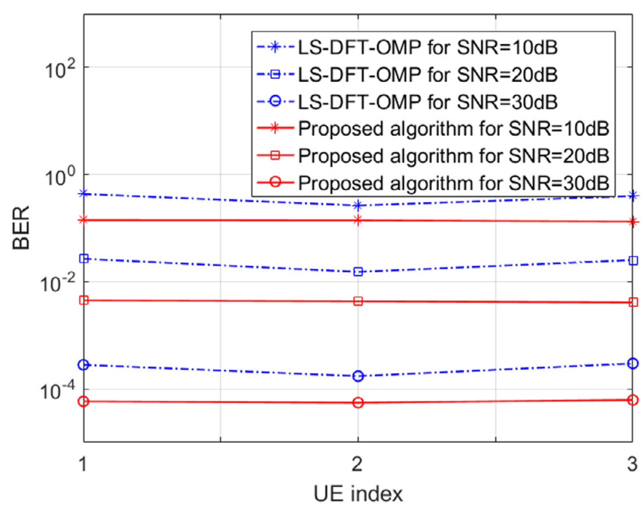

Fig. 9. BER performances for different UE positions.

property of the proposed algorithm is desirable since it eventually translates to a near-uniform quality of communication services throughout the room.

5. Conclusions

In this paper, an adaptive sparse LS channel estimation algorithm was proposed for DCO-OFDM systems. The design of the proposed algorithm was based on the channel tap detection that can maximize the probability of separating non-zero taps out of the channel estimates, thus leading to a superior performance. In addition, the CRLB of the proposed algorithm was proven to be lower than that of the conventional LS algorithm. The simulation results further showed that the proposed algorithm has better performances in terms of the received constellation, MSE and BER than the existing algorithm.

Declaration of competing interest

The authors declare that they have no known competing financial interests or personal relationships that could have appeared to influence the work reported in this paper.

Acknowledgments

The work was supported by the National Natural Science Foundation of China (Project No. 71401134; 71571144; 71171164) and the Program of International Cooperation and Exchanges in Science and Technology Funded by Shaanxi Province, China (Project No. 2016KW-033). The authors are very grateful to the anonymous referees for their detailed comments and suggestions regarding this paper.

References

[1] L.E.M. Matheus, A.B. Vieira, L.F.M. Vieira, M.A.M. Vieira, O. Gnawal, Visible light communication: concepts, applications and challenges, IEEE Commun. Surv. Tutor. 21 (4) (2019) 3204–3237.

[2] T. Hwang, C. Yang, G. Wu, S. Li, G.Y. Li, OFDM and its wireless applications: A survey, IEEE Trans. Veh. Technol. 58 (4) (2009) 1673–1694.

[3] M.M.A. Mohammed, C. He, J. Armstrong, Performance analysis of ACO-OFDM and DCO-OFDM using bit and power loading in frequency selective optical wireless channels, in: IEEE 85th Vehicular Technology Conference, VTC Spring, 2017, pp. 1–5.

[4] S.J. Lee, J.K. Kwon, S.Y. Jung, Evaluation of visible light communication channel delay profiles for automotive applications, EURASIP J. Wireless Commun. Netw. 2012 (1) (2012) 1–8.

[5] W. Xiao, H.G. Deng, F.Q. Jiang, K.C. Zhu, L.Z. Yin, Peak to average power ratio reduction in orthogonal frequency division multiplexing visible light communications system using a combination of a genetic algorithm and a hill-climbing algorithm, Opt. Eng. 54 (3) (2015) 036106.

[6] O. Şayli, H. Doğan, E. Panayirci, On channel estimation in DC biased optical OFDM systems over VLC channels, in: IEEE International Conference on Advanced Technologies for Communications, ATC, 2016, pp. 147–151.

[7] J.C. Estrada-Jiménez, B.G. Guzmán, M.J.F. García, V.P.G. Jiménez, Superimposed training-based channel estimation for MISO optical-OFDM VLC, IEEE Trans. Veh. Technol. 68 (6) (2019) 6161–6166.

[8] A. Özmen, H. Şenol, Channel estimation for realistic indoor optical wireless communication in ACO-OFDM systems, Wirel. Pers. Commun. 102 (1) (2018) 247–259.

[9] V. Suseela, V.V. Mani, Channel estimation in ACO-OFDM employing different transforms for VLC, AEU-Int. J. Electron. Commun. 84 (2018) 111–122.

[10] B. Aly, Performance analysis of adaptive channel estimation for U-OFDM indoor visible light communication, in: 33rd National Radio Science Conference, NRSC, 2016, pp. 217–222.

[11] R. Mulinde, K.D. Nguyen, W.G. Cowley, Analytical estimation schemes for optical unipolar OFDM transmission over AWGN, in: IEEE International Conference on Communications, ICC, 2017, pp. 1–6.

[12] W.F. Lin, C.W. Chow, C.H. Yeh, Using specific and adaptive arrangement of grid-type pilot in channel estimation for white-light LED-based OFDM visible light communication system, Opt. Commun. 338 (2015) 7–10.

[13] X. Qian, H. Deng, H. He, Pilot-based parametric channel estimation algorithm for DCO-OFDM-based visual light communications, Opt. Commun. 400 (2017) 150–155.

[14] T. Foggi, G. Colavolpe, E. Forestieri, G. Prati, Channel estimation algorithms for MLSD in optical communication systems, IEEE Photon. Technol. Lett. 18 (19) (2006) 1984–1986.

[15] W. Chung, Channel estimation methods based on Volterra kernels for MLSD in optical communication systems, IEEE Photon. Technol. Lett. 22 (4) (2010) 224–226.

[16] C. Gong, Z. Xu, Channel estimation and signal detection for optical wireless scattering communication with inter-symbol interference, IEEE Trans. Wirel. Commun. 14 (10) (2015) 5326–5337.

[17] G.D. Forney, The viterbi algorithm, Proc. IEEE 61 (3) (1973) 268–278.

[18] P.A. Haigh, Z. Ghassemlooy, S. Rajbhandari, I. Papakonstantinou, W. Popoola, Visible light communications: 170 Mb/s using an artificial neural network equalizer in a low bandwidth white light configuration, J. Lightw. Technol. 32 (9) (2014) 1807–1813.

[19] C.L. Bai, S. Zhang, S.C. Bai, Q.L. Luo, Development of discrete fourier transform-based channel estimation algorithms for a coherent optical orthogonal frequency division multiplexing transmission system, IET Commun. 8 (14) (2014) 2528–2534.

[20] Y.S. Husseinm, M.Y. Alias, A.A. Abdulkafi, On performance analysis of LS and MMSE for channel estimation in VLC systems, in: IEEE International Colloquium on Signal Processing & its Applications, ICSPA, 2016, pp. 204–205.

[21] H. Zhao, M. Li, R. Wang, Compressed sensing theory-based channel estimation for optical orthogonal frequency division multiplexing communication system, Opt. Commun. 3 (26) (2014) 94–99.

[22] T. Zhang, S.X. Guo, H.P. Chen, F. Zhong, C.Y. Ma, Enhancing the bit error rate of indoor visible light communication systems using adaptive channel estimation algorithm, IET Commun. 9 (4) (2015) 501–507.
[23] C. Chen, D.A. Basnayaka, H. Haas, Downlink performance of optical attocell networks, J. Lightw. Technol. 34 (1) (2016) 137–156.
[24] F. Wan, U. Mitra, A. Molisch, The modified iterative detector/estimator algorithm for sparse channel estimation, in: MTS/IEEE Oceans'2010, 2010, pp. 1–6.
[25] S.M. Kay, Fundamentals of Statistical Signal Processing, Prentice Hall, Upper Saddle River, New Jersey, 2001.